



OPEN Trajectory analysis and optimization of sea buckthorn fruit vibration separation manipulator based on I-PSO algorithm

Bingqin Liang, Xinzhang Lin, Ganghui Liu, Jin Lei & Weibing Wang

In this paper, the optimal time planning of vibration separation trajectory of *Hippophae rhamnoides* fruit is studied for space manipulator using the I-PSO algorithm. The first step is to analyze the motion of the robotic arm's joints, which are limited in range and speed, in combination with a 3–5–3 polynomial interpolation, an improved Particle swarm optimization with adaptive inertia weight and asynchronous learning factor is proposed, and the specific process is given. Experimental images and data show that the improved particle swarm optimization algorithm can ensure the continuity of joint acceleration and velocity, and the optimal vibration trajectory time is 0.536539094 s Compared with the planned system trajectory time of 0.71022 s, the speed increased by 24.5%. The results of the orthogonal experiment show that the average fruit drop rate reaches 96.19%, which verifies the validity and reliability of the I-PSO algorithm for optimal time planning of seabuckthorn fruit separation vibration trajectory.

Sea buckthorn (*Hippophae rhamnoides* L.), also known as vinegar willow, blackthorn; elaeagnaceae sea buckthorn, is known as the 'shining horse' by Greece^{1–3}. The root of sea buckthorn is resistant to cold, drought, and barrenness due to nitrogen fixation by rhizobia, a high-quality ecological tree species for improving soil and the ecological environment^{4–6}. Due to its strong attachment, mature fruit can be crushed by small external forces, resulting in very difficult harvesting. Mechanical harvesting has become a bottleneck problem restricting the large-scale industrial production of the sea buckthorn industry⁷. Among them, the vibration trajectory analysis and optimization methods of the manipulator are very important to realize the mechanization of vibration separation of sea buckthorn fruit.

Time trajectory planning of a manipulator is a process of determining the trajectory of a manipulator under given tasks and constraints. It is very important to ensure safety, improve efficiency, improve precision, adapt to dynamic environments and realize coordinated motion. The time trajectory planning of manipulators is related to the limitation of time efficiency of enterprises and is also an important research point in robot kinematics^{8–11}. Hector et al. simulated and predicted the vibration behavior of fruit by finite element analysis, which provided a theoretical basis for further improving fruit sorting equipment and technology¹². Torregrosa et al. used artificial vision techniques to record the movement of fruits during vibration using a camera under the condition of applying vibration, and extracted the separation effect of citrus fruits by image processing and analysis techniques¹³. To optimize the trajectory of the manipulator, Yong et al. put forward a genetic algorithm optimization method based on a transition rectangle¹⁴. Yan Li et al. applied the coordinated motion characteristics of biology to the motion planning of a manipulator in two-dimensional space and proposed a new biological method to plan the motion of an artificial manipulator¹⁵. Hao Tian et al. proposed a neural network-based trajectory planning method for robotic manipulators and verified the feasibility and effectiveness of the method through several experiments¹⁶. The above research has made a great contribution to the research of trajectory planning and optimization of manipulator. At the same time, we can see that the multi-objective optimization method is not perfect, and the traditional particle swarm optimization algorithm is easy to fall into the local optimization, resulting in slow

College of Mechanical and Electrical Engineering; Xinjiang Production and Construction Corps Key Laboratory of Modern Agricultural Machinery; Key Laboratory of Northwest Agricultural Equipment, Ministry of Agriculture and Rural Affairs, Shihezi University, Shihezi 832003, China. email: wwbshz@163.com

convergence speed, local optimization imbalance and so on. Therefore, in order to solve the problem that traditional algorithms can easily fall into the local optimum, this study chooses to analyze the branch picking and the vibration separation trajectory of seabuckthorn, and optimizes the trajectory time through the improved PSO algorithm. It provides an experimental basis for studying the vibration separation trajectory of sea buckthorn fruit, improves the working efficiency and reliability of the manipulator used for vibration separation of sea buckthorn fruit, improves the production environment, and promotes the development and progress of robot technology.

Materials and methods

Materials

Seabuckthorn comes from the Xinjiang production and Construction Corps 9th Division 170th Regiment Seabuckthorn planting base. The variety is the “Late autumn red” variety whose tree age is about 4 years. The plant-row spacing is about 2–4 m, the plant height is about 2–2.5 m, the width is about 2 m.

Methods

Trajectory analysis

Select the trajectory planning method. Trajectory planning is divided into joint space trajectories and task space trajectories. Angle-space trajectory: first, the angle of two time points in $t_0 \sim t_1$ is interpolated to ensure the continuity of the angle, and then the inverse kinematics trajectory planning of the angle interpolation. Task space trajectory: firstly, interpolate the position displacement from $t_0 \sim t_1$ to ensure the consistency of the displacement, then plan the inverse kinematics trajectory of the position in space.

Since the robot arm can determine the position of the mission space at an unknown joint angle, this research chooses the mission space method for trajectory planning.

Pick up trajectory planning. The JTRAJ function generates robot trajectories quickly and smoothly. The continuous polynomial trajectories generated by the Trajectory of joint space (JTRAJ) function can realize the drop of branches and leaves in the picking process. The joint position at the time point was obtained by entering the starting position, the ending position, and the time step, and the planned trajectory was obtained¹⁷. This trajectory ensures continuity of joint acceleration and velocity, more in line with actual robot motion.

It can be found from Fig. 1. that the JTRAJ function is smooth when planning the pick-up trajectory, and there is a slight vibration of the trajectory, which is beneficial to the drop of branches and leaves during the pick-up process.

Vibration trajectory planning. The path planning of seabuckthorn fruit vibration separation is to make the system vibrate according to the predetermined path or path through reasonable design and control.

The joint space and mission space trajectory planning points for the seabuckthorn fruit vibration separation manipulator were set to (0, 0, 0.2), (−0.1, 0.2, 0.4), (−0.2, 0, 0.1), (−0.1, −0.2, 0.4), (−0.1, −0.2, 0.4), (−0.1, −0.2, 0.4), (−0.1, −0.2, 0.4), the last loop returns at the initial position (0,0,0.2). The simulation results are shown in Fig. 2.

As shown in Fig. 3, the space trajectory time required for the joint task is 0.71022 s, and the joint angle trajectory planning time is 0.13634 s. From Fig. 4, it can be seen that the whole trajectory planning of the mission space is smooth, the angle space trajectory planning is direct, the trajectory changes greatly, and has certain impact on the manipulator.

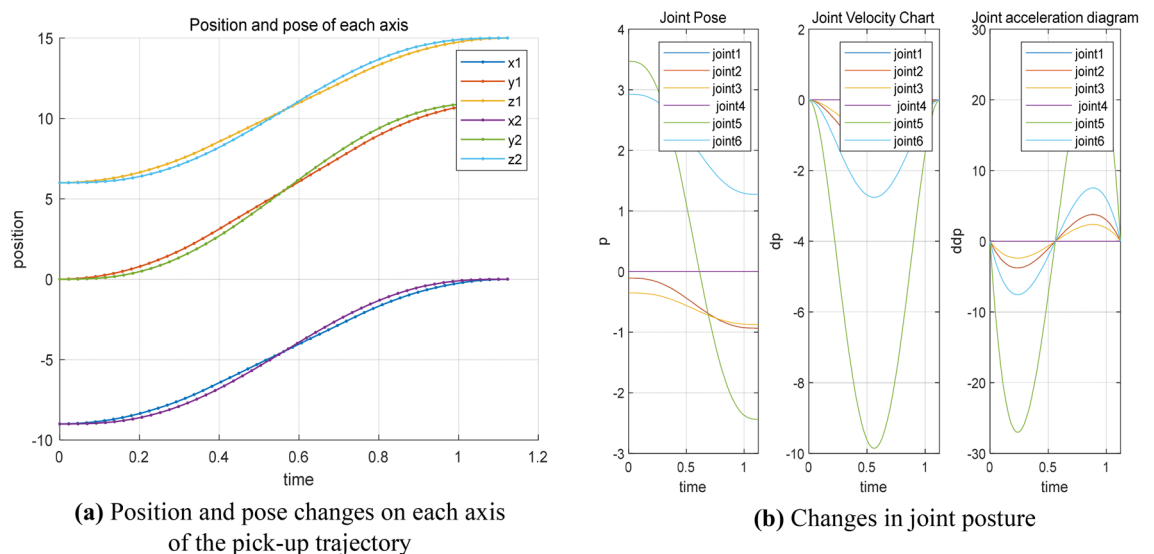


Figure 1. JTRAJ function is used to pick up the parameters of the robot arm.

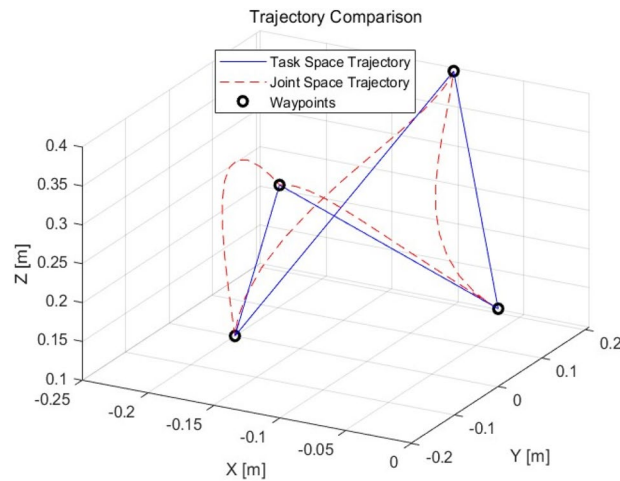


Figure 2. Trajectory of joint angle and task space angle.

Time optimization of vibration trajectory based on I-PSO algorithm

Particle swarm optimization. Particle Swarm Optimization (PSO) is a swarm-intelligent global stochastic search algorithm that simulates flocks' migration, foraging behavior, and fuses concepts of social psychology such as individual cognition and social influence¹⁸, a member of Evolutionary Algorithm-EA, abbreviated PSO¹⁹.

Particle swarm velocity update Formula:

$$V_{id}^{k+1} = WV_{id}^k + C_1 r_1 (P_{id,pbest}^k - X_{id}^k) + C_2 r_2 (P_{d,gbest}^k - X_{id}^k) \quad (1)$$

i : Particle number; d : Particle dimension number; k : Number of iterations; W : Inertia weight; c_1 : Individual learning factors; c_2 : Group learning factor; r_1, r_2 : A random number in an interval $[0, 1]$; V_{id}^k : The d -dimensional velocity vector of particle i in the k -th iteration; X_{id}^k : The d -dimensional position vector of particle i in the k -th iteration; $P_{id,pbest}^k$: The historical optimal position of particle i in d -dimension in the k -th iteration; $P_{d,gbest}^k$: The historical optimal position of the d -dimension in the k -th iteration.

WV_{id}^k (Inertial part): by the inertia weight and the particle's speed, indicating the particle's previous state of trust in their motion. $C_1 r_1 (P_{id,pbest}^k - X_{id}^k)$ (Individual Cognition): the self-cognition of a particle, that is, the part of the particle's own experience, which can be understood as the distance and direction between the current position of the particle and the optimal position in the individual's history. $C_2 r_2 (P_{d,gbest}^k - X_{id}^k)$ (Social sharing): information sharing and cooperation between particle swarm, that is, the experience of optimization from other particles in the swarm, can be understood as the distance and direction between the current position of the particle and the historical optimal position of the swarm.

Improved particle swarm optimization algorithm (I-PSO). The inertia weight w and learning factors C_1, C_2 , and other parameters of the traditional particle swarm optimization algorithm are fixed. In the optimization process, the algorithm is prone to fall into the local optimal trap and other problems, resulting in slow convergence, local optimization imbalance, and global optimization errors²⁰. When using the PSO algorithm to plan the optimal time of the manipulator, it is necessary to ensure the constraint of the velocity boundary of the manipulator's joint and the continuity of the acceleration. Therefore, in this paper, the motion time of the manipulator is optimized by introducing adaptive inertia weight, asynchronous learning factor, and 3–5–3 polynomial interpolation Particle Swarm Optimization. The improved particle swarm optimization algorithm is abbreviated as I-PSO.

Adaptive inertia weight W :

$$W = W_{max} - (W_{max} - W_{min}) e^{\left(\frac{4k}{N_{max}}\right)^2} \quad (2)$$

k, N_{max} : The current and maximum values for the number of iterations, respectively; W_{max}, W_{min} : The maximum and the minimum of the inertia weight.

In particle swarm optimization, inertia weight W can balance the global and local optimization ability and convergence speed by controlling the size of search area²¹. When a larger inertia weight W is used, the inertia of particle motion and the ability of searching the extended space are enhanced, which is beneficial to the global optimization, jumping out of the local extremum and not falling into the local optimum, the local optimization ability will be enhanced, which enables the algorithm to converge to the optimal solution quickly²². The traditional PSO algorithm only increases or decreases the inertia weight, and cannot cope with the changing demand in the complex real-life environment. Therefore, this paper introduces an adaptive inertia weight that can achieve different weights at different stages according to the complex search case, as shown in Formula (2). In the early stage of the PI-PSO algorithm, due to the large problem space, to ensure the balance of search speed and precision, the larger inertia weight is used in the early stage of PI-PSO algorithm to reach the higher global

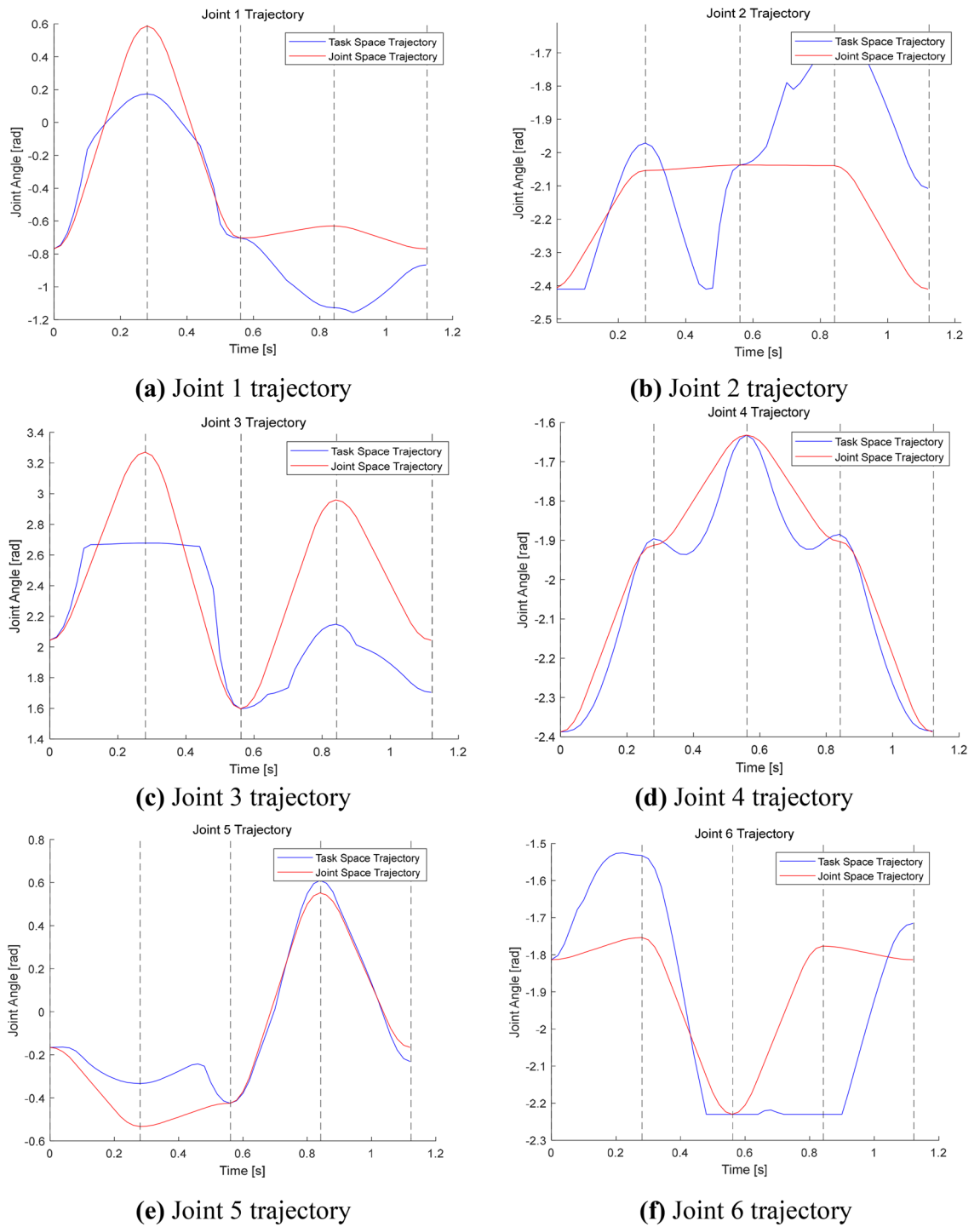


Figure 3. The vibration track of each joint of the manipulator.

search ability to obtain the correct solution. At a later stage, the local search capability is improved by using smaller inertia weights to improve convergence accuracy.

Asynchronous learning factor C_1, C_2 :

$$C_1 = \frac{(C_{1f} - C_{1i})k}{N_{max}} + C_{1i} \tag{3}$$

$$C_2 = \frac{(C_{2f} - C_{2i})k}{N_{max}} + C_{2i} \tag{4}$$

C_1 : Acceleration coefficient of individual cognition; C_2 : Accelerated coefficient of social sharing.

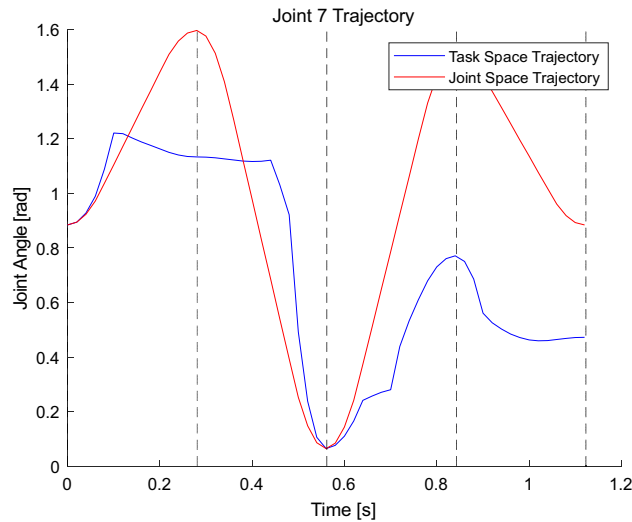


Figure 4. The end of the manipulator clamps the track of the component.

From the Formula (1), we know that the learning factor C_1 affects the “Individual cognition” ability of the particle, and it should decrease gradually with the increase of the number of search iterations, while the learning factor C_2 affects the “Social sharing” ability of the particle, it should increase as the number of search iterations increases. Since the learning factors C_1 and C_2 of traditional particle swarm optimization are fixed, this will affect the algorithm’s optimization speed and solution accuracy balance. Therefore, asynchronous learning factors are introduced in this paper, as shown in Formulas (3) and (4). In the early stage of optimization, the improved algorithm ensures that the region of the initial individual cognitive solution is larger than that of the group cognitive solution and that the particles do not fall into the local extremum trap, it makes the group have a strong global optimization ability and convergence speed.

3–5–3 Polynomial interpolation:

$$h_{i1}(t)h_{i1}(t) = a_{i13}t^3 + a_{i12}t^2 + a_{i11}t^1 + a_{i10} \tag{5}$$

$$h_{i2}(t) = a_{i25}t^5 + a_{i24}t^4 + a_{i23}t^3 + a_{i22}t^2 + a_{i21}t^1 + a_{i20} \tag{6}$$

$$h_{i3}(t) = a_{i33}t^3 + a_{i32}t^2 + a_{i31}t^1 + a_{i30} \tag{7}$$

$h_{im}(t)$: The trajectory function of the m time segment of the i joint; a_{imj} represents the j -segment coefficient of the m -segment interpolation function for the i -segment articulation trajectory. The matrix form of the coefficient is shown in Formula (9), and Formula (8) is the coefficient solution.

$$b = [0, 0, 0, 0, 0, 0, X_3, 0, 0, X_0, 0, 0, X_2, X_1]^T \tag{8}$$

$$A = \begin{bmatrix} t_1^3 & t_1^2 & t_1 & 1 & 0 & 0 & 0 & 0 & 0 & -1 & 0 & 0 & 0 & 0 \\ 3t_1^2 & 2t_1 & 1 & 0 & 0 & 0 & 0 & 0 & -1 & 0 & 0 & 0 & 0 & 0 \\ 6t_1 & 2 & 0 & 0 & 0 & 0 & 0 & -2 & 0 & 0 & 0 & 0 & 0 & 0 \\ 0 & 0 & 0 & 0 & t_2^5 & t_2^4 & t_2^3 & t_2^2 & t_2 & 1 & 0 & 0 & 0 & -1 \\ 0 & 0 & 0 & 0 & 5t_2^4 & 4t_2^3 & 3t_2^2 & 2t_2 & 1 & 0 & 0 & 0 & 0 & -1 \\ 0 & 0 & 0 & 0 & 20t_2^3 & 12t_2^2 & 6t_2 & 2 & 0 & 0 & 0 & -2 & 0 & 0 \\ 0 & 0 & 0 & 0 & 0 & 0 & 0 & 0 & 0 & 0 & t_3^3 & t_3^2 & t_3 & 1 \\ 0 & 0 & 0 & 0 & 0 & 0 & 0 & 0 & 0 & 0 & 3t_3^2 & 2t_3 & 1 & 0 \\ 0 & 0 & 0 & 0 & 0 & 0 & 0 & 0 & 0 & 0 & 6t_3 & 2 & 0 & 0 \\ 0 & 0 & 0 & 1 & 0 & 0 & 0 & 0 & 0 & 0 & 0 & 0 & 0 & 0 \\ 0 & 0 & 1 & 0 & 0 & 0 & 0 & 0 & 0 & 0 & 0 & 0 & 0 & 0 \\ 0 & 1 & 0 & 0 & 0 & 0 & 0 & 0 & 0 & 0 & 0 & 0 & 0 & 0 \\ 0 & 0 & 0 & 0 & 0 & 0 & 0 & 0 & 0 & 0 & 0 & 0 & 0 & 1 \\ 0 & 0 & 0 & 0 & 0 & 0 & 0 & 0 & 0 & 1 & 0 & 0 & 0 & 0 \end{bmatrix} \tag{9}$$

$$B = inv(A) \tag{10}$$

$$H = B * b \tag{11}$$

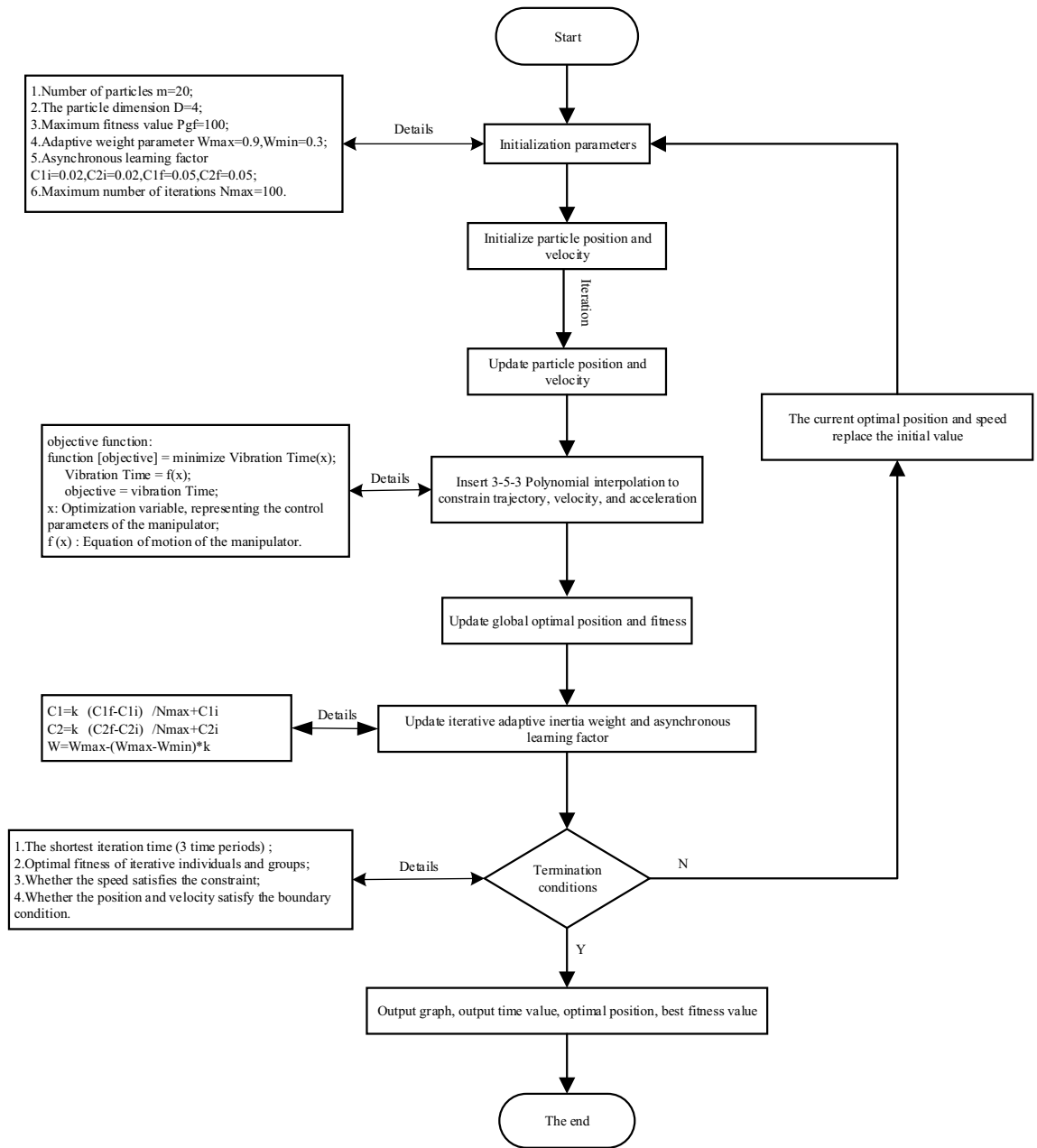


Figure 5. I-PSO algorithm flow chart.

b: A coefficient containing an unknown number; A: A simple function of time; H: The motion matrix of the manipulator with respect to time T.

(I-PSO) algorithm target content description (flowchart). The flow chart of the improved I-PSO algorithm is shown in Fig. 5. The I-PSO algorithm is based on traditional particle swarm optimization (PSO-RRB-algorithm). By improving adaptive inertia weight and asynchronous learning factor, Polynomial interpolation between optimization speed and precision can be ensured.

Methodology statement

This study states that the experiment and simulation of the vibration trajectory of the manipulator, including the collection of Hippophae rhamnoides materials, are in line with relevant institutions, national and international standards.

Results

According to the experimental data of Supplementary materials, the optimization results of each axis near the optimal time in the simulation experiment are shown as follows: the trajectory planning of the manipulator on the X-axis by multi-group simulation experiments is closest to the experimental average value as shown in Fig. 6.

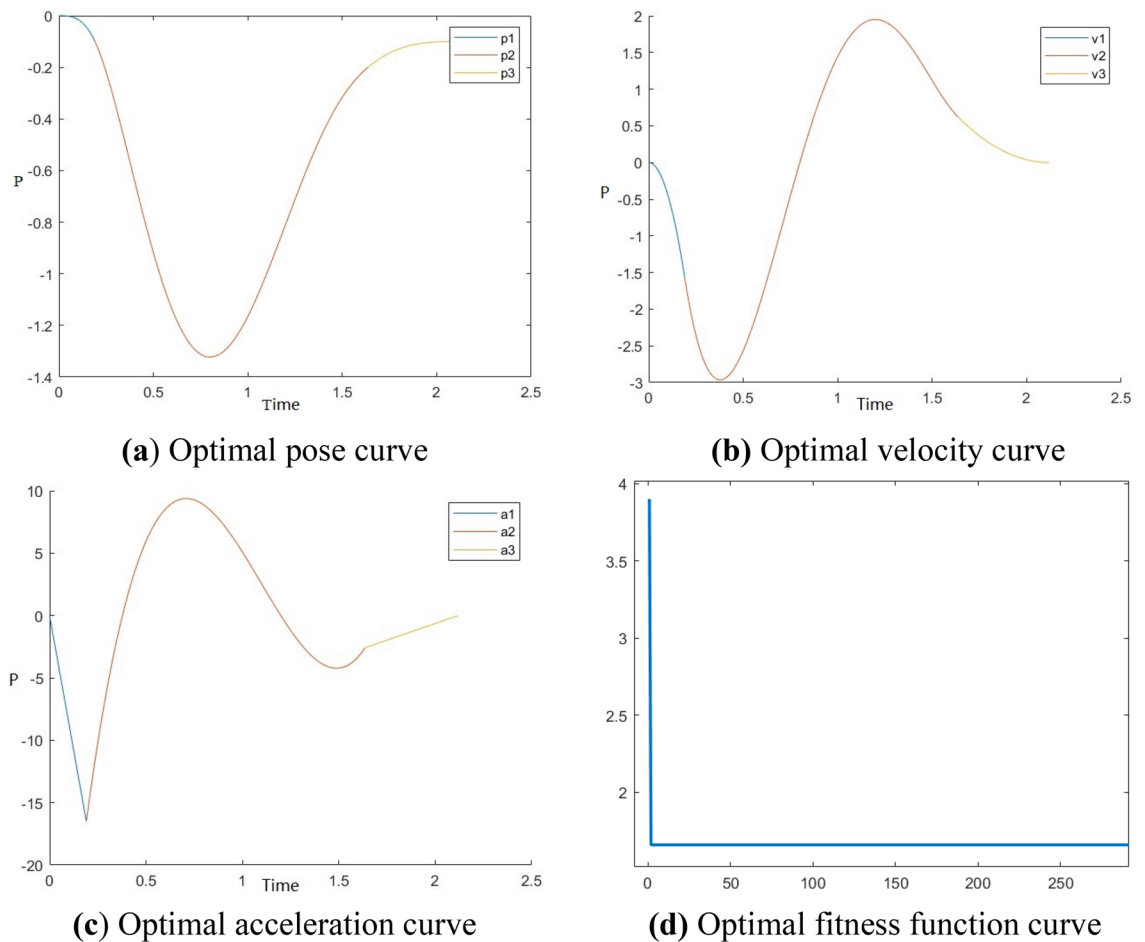


Figure 6. Optimal time trajectory planning of manipulator on X-axis.

The trajectory planning of the manipulator on the Y-axis is most close to the experimental average through several simulation experiments, as shown in Fig. 7. The trajectory planning of the manipulator on the Z-axis is most close to the experimental average through several simulation experiments, as shown in Fig. 8.

When the time of the vibration trajectory of the manipulator is optimized by the algorithm, the pose of the X-axis and the Z-axis fluctuates greatly. Four groups of simulation experiments are carried out for optimal time trajectory planning. The results show that one group of experimental data is unqualified, and the remaining six groups of optimal time are 0.396 s, 0.483 s, 0.735 s and 0.700 s, 0.408 s, 0.498 s. Three groups of simulation experiments were carried out on the Y-axis trajectory, and the optimal time was 0.802 s, 0.539 s, and 0.533 s. The average optimal time of the X-axis is 0.538 s; the average optimal time of the Y-axis is 0.536 s; the average optimal time of the Z-axis is 0.535 s.

To verify the validity and reliability of the algorithm, the vibration trajectories of Seabuckthorn branches were analyzed by the method of variance analysis. The fruit data of *Hippophae rhamnoides* L. were obtained as shown in Table 1.

SPSS software was used to analyze the fruit drop rate variance, and test tables of inter-body effects were shown in Table 2.

In Table 2, the significance of the modified model is greater than 0.05, so there is no significant difference between the modified model and the whole analysis of the variance model, and the effect is vibration frequency > vibration amplitude > vibration time.

Conclusion

Based on the 3–5–3 Polynomial interpolation function, the vibration trajectory of *Hippophae rhamnoides* is optimized in time by using an improved Particle swarm optimization system (I-PSO), the results of the simulation experiment are as follows:

- (1) In this study, the trajectory planning of mission space can realize the drop of branches and leaves in the process of picking up and can ensure the continuity of joint pose, velocity, and acceleration of the trajectory, much closer to the actual movement of the robot.
- (2) In this study, an improved particle swarm optimization (PSO-RRB-algorithm combined with 3–5–3 Polynomial interpolation is used to select the optimal time for the manipulator to complete the motion

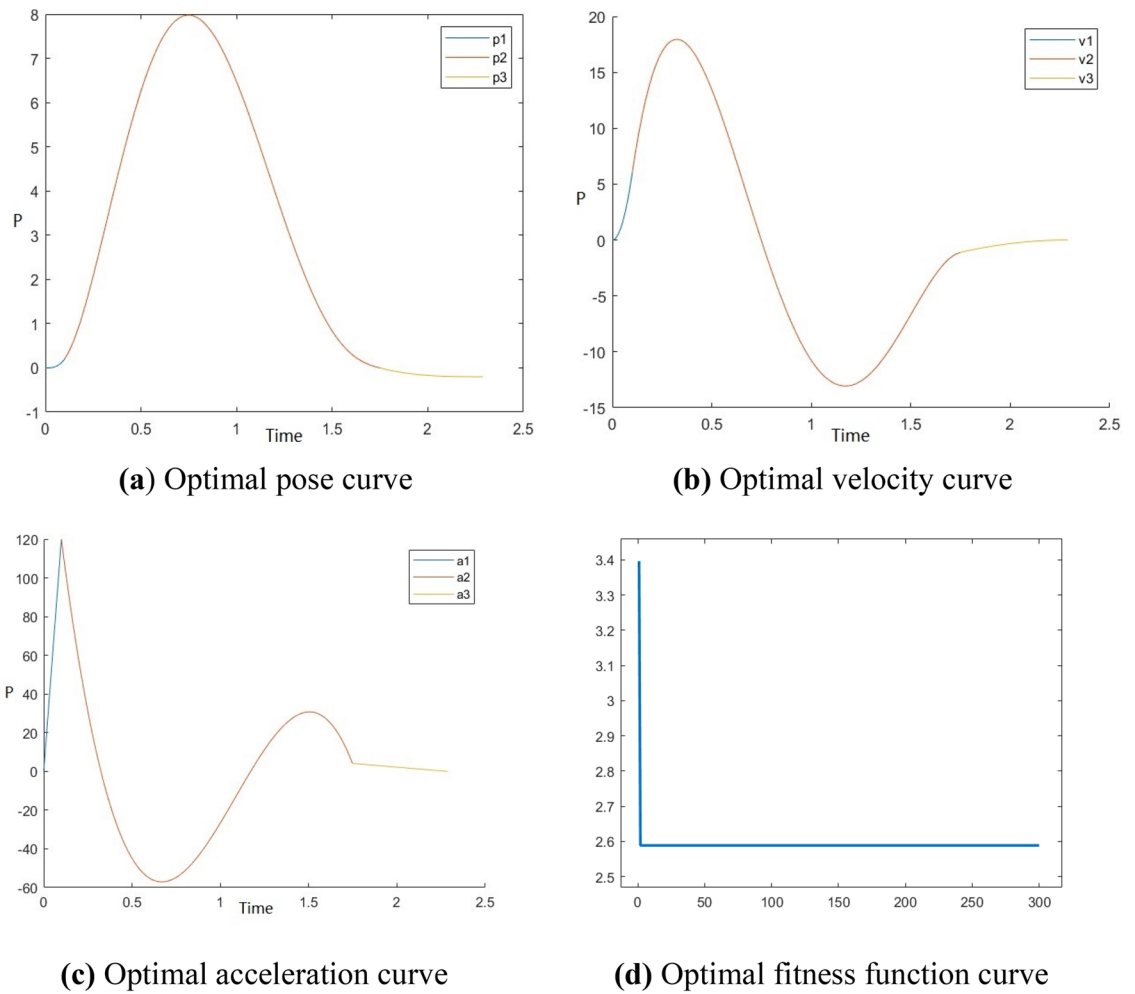


Figure 7. Optimal time trajectory planning of manipulator on Y-axis.

in the shortest time and satisfy the speed constraint, the simulation results show that the average optimal linkage time is 0.536539094 s, which is 24.5% higher than the original trajectory time 0.71022 s planned by JTRAJ function. The effectiveness and superiority of the I-PSO algorithm for time trajectory optimization are proved. Contribute to the development of research on trajectory planning and optimization of related manipulators. The utility model can be used for reducing the movement time of the mechanical arm and improving the work efficiency of seabuckthorn fruit collection. The optimization of traditional algorithms is convenient to promote the development of artificial intelligence. The trajectory also ensures the continuity of the robot's terminal posture.

- (3) SPSS was used to analyze the variance of the vibration orthogonal test of seabuckthorn branches. The data show that the average fruit drop rate of the optimized algorithm can reach 96.19%, which is 0.87% higher than the 95.32% average fruit drop rate of the original JTRAJ function trajectory planning, the validity and reliability of I-PSO algorithm for optimal time planning of seabuckthorn fruit separation vibration trajectory were verified. But from the experimental data, we can see that the acceleration changes more quickly will have an impact, the later need to study from this aspect.

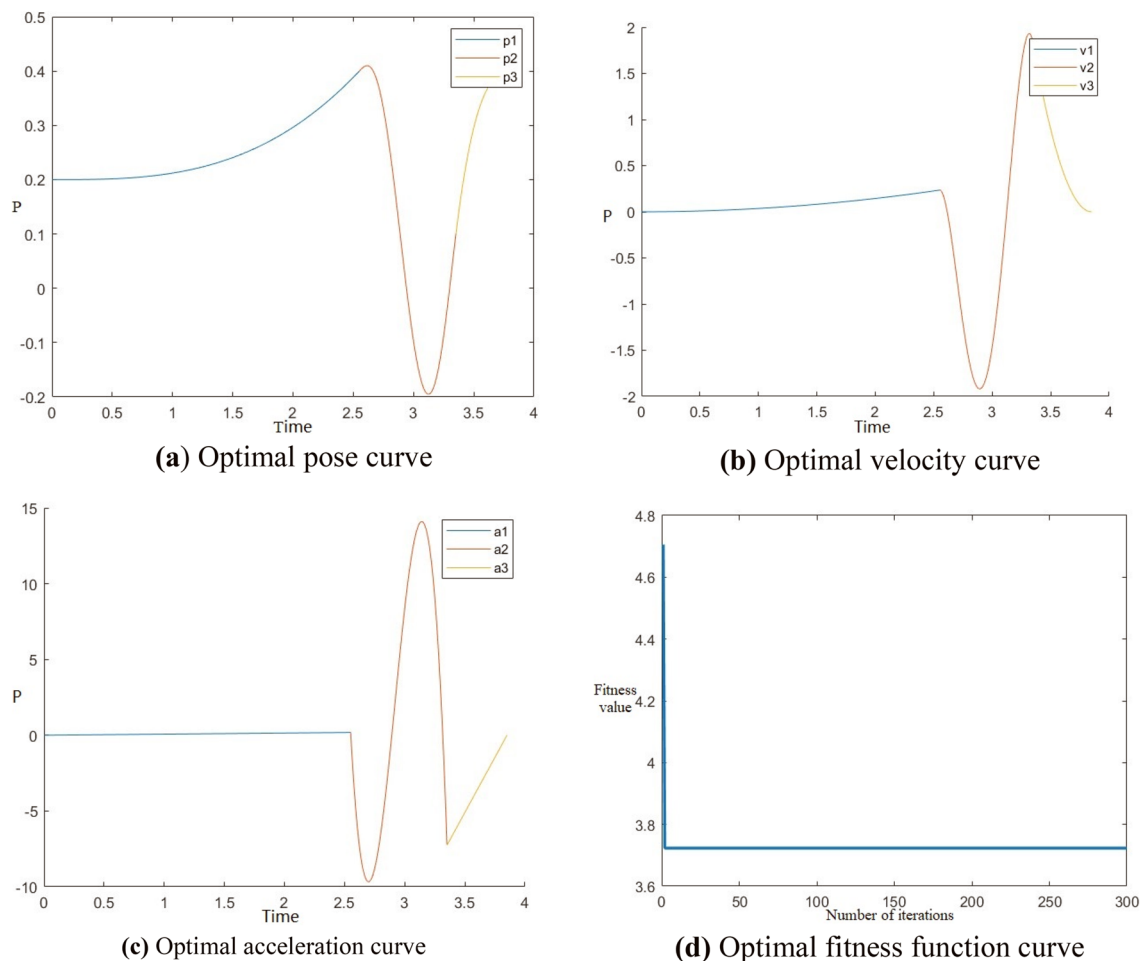


Figure 8. Optimal time trajectory planning of manipulator on Z-axis.

No.	Vibration frequency (Hz)	Amplitude of vibration (mm)	Vibration time (s)	Fruit drop rate	Average fruit drop rate	Optimize the number of fruit drop before	Average fruit drop rate before optimization
1	21.1	30	2	98.84%	98.21%	96.51%	97.05%
2	21.1	30	2	97.59%		97.59%	
3	21.1	30	4	98.94%	99.47%	97.87%	98.31%
4	21.1	30	4	100.00%		98.75%	
5	21.1	20	4	96.51%	96.76%	96.51%	97.26%
6	21.1	20	4	97.00%		98.00%	
7	16.2	30	4	96.55%	96.08%	95.40%	94.40%
8	16.2	30	4	95.60%		93.41%	
9	16.2	30	4	96.70%	96.29%	95.60%	95.74%
10	16.2	30	4	95.88%		95.88%	
11	16.2	20	2	95.51%	95.43%	94.38%	94.87%
12	16.2	20	2	95.35%		95.35%	
13	14.4	30	4	94.62%	95.18%	93.55%	94.65%
14	14.4	30	4	95.74%		95.74%	
15	14.4	30	2	94.74%	94.14%	94.74%	92.53%
16	14.4	30	2	93.55%		90.32%	
17	14.4	20	4	93.81%	94.16%	92.78%	93.10%
18	14.4	20	4	94.51%		93.41%	

Table 1. Experimental data of Hippophae rhamnoides L.

Source	Class III sum of squares	Degree of freedom	Mean square	F	P
Modify the model	0.003 ^a	7	0	159.763	0.061
Intercept	7.029	1	7.029	3,135,621.505	0
Vibration frequency (Hz)	0.002	2	0.001	413.748	0.035
Amplitude of vibration/mm	0	1	0	155.711	0.051
Vibration time (s)	0	1	0	58.787	0.083
Error	2.24E-06	1	2.24E-06		
Total	8.33	9			
Corrected total	0.003	8			

Table 2. Inter-body effect test of fruit drop rate. ^aR Square = 0.999(Adjusted R Square = 0.993).

Data availability

All data generated or analyzed during this study are included in this published article and its Supplementary information files.

Received: 1 May 2023; Accepted: 7 November 2023

Published online: 17 November 2023

References

- Pundir, S. *et al.* Ethnomedicinal uses, phytochemistry and dermatological effects of *Hippophae rhamnoides* L.: A review. *J. Ethnopharmacol.* **266**, 113434 (2021).
- Surmiński, J. Występowanie i właściwości rokitnika zwyczajnego (*Hippophae rhamnoides* L.). *Sylwan* **152**(4), 68–74 (2008).
- Liu, X. *et al.* Study on the stability of sea buckthorn cloudy juice. *China Brewing* **37**(6), 136–139 (2018).
- Liu, G. X. The origin of the Latin name of *Hippophae rhamnoides* L. *China Health Food* **10**, 80 (2018).
- Gátlán, A. M. & Gutt, G. Sea buckthorn in plant based diets. An analytical approach of sea buckthorn fruits composition: Nutritional value, applications, and health benefits. *Int. J. Environ. Res. Public Health* **18**(17), 8986 (2021).
- Bonciu, E. *et al.* Cytogenetic study on the biostimulation potential of the aqueous fruit extract of *Hippophae rhamnoides* for a sustainable agricultural ecosystem. *Plants* **9**(7), 843 (2020).
- Yan, D. *et al.* Vibration analysis and experimental study of the effects of mechanised grape picking on the fruit–stem system. *Biosyst. Eng.* **227**, 82–94 (2023).
- Tong, H. Y. *et al.* Research on pipe and bar unbundling robot system and trajectory planning. *Combin. Mach. Tool Autom. Mach. Technol.* **7**, 40–43 (2022).
- Chen, H. *et al.* A time optimal trajectory planning method for offshore cranes with ship roll motions. *J. Franklin Inst.* **359**(12), 6099–6122 (2022).
- Abu-Dakka, F. J. *et al.* Statistical evaluation of an evolutionary algorithm for minimum time trajectory planning problem for industrial robots. *Int. J. Adv. Manuf. Technol.* **89**, 389–406 (2017).
- Okuyama, I. F., Maximo, M. R. O. A. & Afonso, R. J. M. Minimum-time trajectory planning for a differential drive mobile robot considering non-slipping constraints. *J. Control Autom. Electr. Syst.* **32**(1), 120–131 (2021).
- Tinoco, H. A. & Peña, F. M. Finite element analysis of *Coffea arabica* L. var. Colombia fruits for selective detachment using forced vibrations. *Vibration* **1**(1), 207–219 (2018).
- Torregrosa, A. *et al.* Analysis of the detachment of citrus fruits by vibration using artificial vision. *Biosyst. Eng.* **119**, 1–12 (2014).
- Yong, G. *et al.* Genetic algorithm optimization based on jumping rectangle in mechanical arm trajectory planning. *J. Phys. Conf. Ser.* **1389**(3), 032041 (2019).
- Li, Y. *et al.* Bio-inspired approach for motion planning of robot manipulators. *Neurocomputing* **312**, 147–155 (2018).
- Tian, H. *et al.* Robotic arm path planning based on neural network. *Intell. Control Autom.* **10**(8), 39–47 (2019).
- Wang, H., Lai, Y. & Chen, W. The time optimal trajectory planning with limitation of operating task for the Tokamak inspecting manipulator. *Fusion Eng. Design* **113**, 57–65 (2016).
- Yuan, J. T., Liu, J. & Zou, S. L. Multi objective optimal trajectory planning of industrial robot based on particle swarm optimization. *Ind. Instrum. Autom.* **5**, 73–79 (2021).
- Kennedy, J. & Eberhart, R. Particle swarm optimization. in *Proceedings of ICNN'95-International Conference on Neural Networks. IEEE*, **4**, 1942–1948 (1995).
- Fan, S. K. S., Liang, Y. & Zahara, E. Hybrid simplex search and particle swarm optimization for the global optimization of multimodal functions. *Eng. Optim.* **36**(4), 401–418 (2004).
- Agrawal, A. & Tripathi, S. Particle swarm optimization with adaptive inertia weight based on cumulative binomial probability. *Evol. Intell.* **14**, 305–313 (2021).
- Nickabadi, A., Ebadzadeh, M. M. & Safabakhsh, R. A novel particle swarm optimization algorithm with adaptive inertia weight. *Appl. Soft Comput.* **11**(4), 3658–3670 (2011).

Author contributions

Conceptualization, B.L., and X.L.; methodology, B.L.; software, B.L.; formal analysis, B.L., and X.L.; investigation, B.L.; resources, B.L.; data curation, B.L., and X.L.; writing-original draft preparation, B.L.; writing-review and editing, B.L., X.L., G.L., J.L., W.W.; B.L. developed and validated the proposed method; supervision, W.W. All authors have read and agreed to the published version of the manuscript.

Funding

National and Regional Science Foundation of China (Project No.: 62163032); Financial Science and Technology Plan of Xinjiang Construction Corps (Project No.: 2022CB011); Science and Technology special project of the 9th Division of Xinjiang Construction Corps, research on key technologies for sea buckthorn fruit harvesting and development of supporting equipment (Project No.: 2021JS008).

Competing interests

The authors declare no competing interests.

Additional information

Supplementary Information The online version contains supplementary material available at <https://doi.org/10.1038/s41598-023-47001-2>.

Correspondence and requests for materials should be addressed to W.W.

Reprints and permissions information is available at www.nature.com/reprints.

Publisher's note Springer Nature remains neutral with regard to jurisdictional claims in published maps and institutional affiliations.



Open Access This article is licensed under a Creative Commons Attribution 4.0 International License, which permits use, sharing, adaptation, distribution and reproduction in any medium or format, as long as you give appropriate credit to the original author(s) and the source, provide a link to the Creative Commons licence, and indicate if changes were made. The images or other third party material in this article are included in the article's Creative Commons licence, unless indicated otherwise in a credit line to the material. If material is not included in the article's Creative Commons licence and your intended use is not permitted by statutory regulation or exceeds the permitted use, you will need to obtain permission directly from the copyright holder. To view a copy of this licence, visit <http://creativecommons.org/licenses/by/4.0/>.

© The Author(s) 2023